Langmuir

Article

pubs.acs.org/Langmuir

Phospholipid/Aromatic Thiol Hybrid Bilayers

Chao Li, Mingming Wang, Matthew Ferguson, and Wei Zhan*

Department of Chemistry and Biochemistry, Auburn University, Auburn, Alabama 36849, United States

Supporting Information

ABSTRACT: Gold-supported hybrid bilayers comprising phospholipids and alkanethiols have been found to be highly useful in biomembrane mimicking as well as biosensing ever since their introduction by Plant in 1993 (Plant, A. L. *Langmuir* **1993**, *9*, 2764−2767). Generalizing the mechanism (i.e., hydrophobic/hydrophobic interaction) that primarily drives bilayer formation, we report here that such a bilayer structure can also be successfully obtained when aromatic thiols are employed in place of alkanethiols. Four aromatic thiols were studied here (thiophenol, 2-naphthalene thiol, biphenyl-4-thiol, and diphenylenevinylene methanethiol), all affording reliable bilayer formation when 1-palmitoyl-2-oleoyl-*sn*-glycero-3-phosphocholine liposomes were incubated with self-assembled monolayers of these thiols. Characterization of the resultant structures, using cyclic voltammetry, impedance analysis, and atomic force microscopy, confirms the bilayer formation. Significant differences in electrochemical blocking and mechanical characteristics of these new bilayers were identified in comparison to their alkanethiol counterparts. Taking advantage of these new features, we present a new scheme for the straightforward biorecognition of a lipolytic enzyme (phospholipase A_2) using these phospholipid/aromatic thiol bilayers.

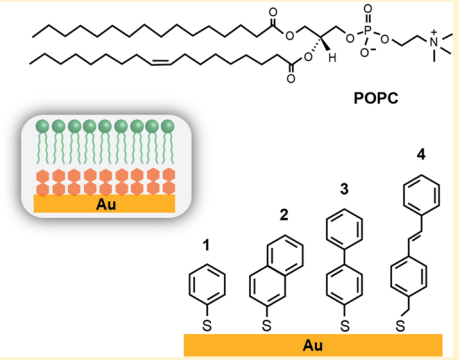

INTRODUCTION

In 1993, Plant first demonstrated that a monolayer of phospholipids could be reliably placed on an alkanethiol self-assembled monolayer (SAM) anchored on gold to produce a stable hybrid bilayer structure.[1] While the top lipid layer reserves much utility of such structures as biomembrane mimics,[2] their direct interface with gold enables many optical, electrical, and electrochemical techniques[3−5] to be used for characterization and detection. Since then, these lipid/alkane hybrid bilayers have grown into a valuable biomembrane platform[6,7] in fundamental as well as applied studies of lipid-based surfaces and interfaces.

Many important characteristics of phospholipid/alkane hybrid bilayers emanate from their unique formation mechanism, which is driven primarily by hydrophobic interaction between the acyl chains of lipids and the alkanethiol SAM.[2,8] In a typical preparation of such a hybrid bilayer, a suspension of small unilamellar liposomes is incubated with a preformed SAM for a certain period of time, during which these lipid colloidal particles diffuse and adhere to the SAM, thereby rupturing and spreading to eventually cover the latter as a complete monolayer. In this complex series of events, the initial energy barrier imposed by liposome rupturing is overcome by the hydrophobic interaction, and the subsequent bilayer formation is thermodynamically favored and stabilized as it not only lowers the surface energy of the aqueous-exposed hydrophobic SAM but also releases the internal mechanical stress of the curved lipid bilayer packed in the form of liposomes.[9,10] Besides alkanethiol SAMs, the successful deposition of a monolayer of lipids on top of aqueous-immersed hydrophobic surfaces has also been observed on surfaces decorated with polymers,[11] silanes,[12] and ferrocene,[13] pointing to the generality of such a formation mechanism.

In this work, we systematically studied the deposition of phospholipids on another type of hydrophobic surface: self-assembled monolayers of aromatic thiols. Considering the differences[14−16] in size, orientation, and packing density between the SAMs formed by aromatic and alkyl thiols, we hope to identify new structural features in these aromatic/lipid based hybrid bilayers. In the long term, we also envision that the prevalence of a delocalized π-electron system in aromatic thiols may potentially enhance the functionality of these hybrid lipid bilayers, e.g., on the basis of improved electrical conductivity or new electronic energy states available in such systems. Four aromatic thiols were investigated here, all of which were found to afford hybrid lipid bilayer formation. The impedance and voltammetric characteristics of these new hybrid films were compared to those of the butanethiol- and dodecanethiol-based bilayers, and atomic force microscopy (AFM) measurements of these films provide further evidence of the lipid/aromatic thiol bilayer formation. A convenient voltammetric biorecognition scheme for a lipid-cleaving enzyme (phospholipase A_2) is introduced at the end, revealing important differences between aromatic- and alkane-based hybrid bilayers.

Received: February 5, 2015
Revised: April 15, 2015
Published: April 21, 2015

ACS Publications © 2015 American Chemical Society

DOI: 10.1021/acs.langmuir.5b00476
Langmuir 2015, 31, 5228−5234

EXPERIMENTAL SECTION

Reagents. 1-Palmitoyl-2-oleoyl-*sn*-glycero-3-phosphocholine (POPC) was purchased from Avanti Polar Lipids (Alabaster, AL). Other chemicals, including potassium hexacyanoferrate(II) trihydrate ($K_4Fe(CN)_6{\cdot}3H_2O$), 1-butanethiol (C4 thiol), 1-dodecanethiol (C12 thiol), thiophenol, biphenyl-4-thiol, 2-naphthalenethiol, 4-(2-hydroxyethyl)piperazine-1-ethanesulfonic acid (HEPES), *trans*-4-stilbenecarboxyaldehyde, triphenylphosphine, thioacetic acid, diethyl azodicarboxylate, and phospholipase A_2 (from honey bee venom *Apis mellifera*), were products of Sigma-Aldrich and used as received. All aqueous solutions employed in this study were prepared using 18.2 MΩ·cm deionized water (Millipore).

Diphenylenevinylene (DPV) methyl thioacetate was synthesized from stilbenecarboxyaldehyde and purified following the procedure reported by Dudek.[17] The identity and purity of the product were confirmed by ^{1}H NMR and GC/MS (calculated, 268.0922; found, 268.1021).

Assembling of Hybrid Bilayers. All monolayers and bilayers studied in this work were formed on gold substrates from two sources. For electrochemical and impedance analysis, the substrates were fabricated in-house by sputtering gold (thickness: ∼1000 nm as determined by quartz crystal microbalance) onto chromium-coated silicon wafers, and for the AFM measurements, gold-coated (thickness: 10 nm) glass substrates from Sigma-Aldrich were directly used. Right before the monolayer formation, these gold substrates were cleaned in piranha solution (3:1 v/v conc H_2SO_4/30% H_2O_2) for 3 or 15 min, with the latter time used for 1000-nm-thick gold-coated substrates. (***Caution!*** *Extreme care should be applied in handling the piranha solution because of its high reactivity toward organic materials.*) These substrates were then thoroughly rinsed with DI water and dried with argon or nitrogen. Thus cleaned gold substrates were immediately immersed in ethanol solutions of aromatic thiols (1−5 mM) at room temperature for at least 15 h to afford monolayer formation. In the case of DPV SAM formation, an additional step was employed in which the acetate group of the DPV methyl thioacetate was first released via base hydrolysis by adding a small amount of concentrated NH_4OH in ethanol.[18] At the end of the incubation, the thiol-attached gold substrates were carefully rinsed with methanol and with DI water, dried in argon or nitrogen, and immediately assembled in various sample holders for electrochemical, impedance, or AFM measurements.

The deposition of lipids on self-assembled monolayers of aromatic thiols was achieved by incubating the monolayer in a POPC liposome solution. The liposomes were prepared by an extrusion-based method described previously[19] in which thoroughly dried POPC films were rehydrated in HEPES buffer and extruded through 400 and 80 nm polycarbonate membranes consecutively. To form a hybrid bilayer comprising phospholipid and aromatic thiol, a certain volume of the liposome solution, with a typical POPC concentration of 2.5 mM, was gently added to an aromatic SAM fixed in the Teflon cell and incubated for 2 h. The unbound liposomes were then removed from the cell by thorough buffer (10 mM HEPES, 100 mM NaCl, pH 7.7) exchange.

Electrochemical Measurements. The electrochemical measurements were performed in homemade Teflon cells housing SAM-covered gold substrates (with or without a deposited lipid layer) as the working electrode, a platinum wire as the counter electrode, and Ag/AgCl in saturated KCl solution as the reference electrode. Cyclic voltammetry of these films was operated by a PC-controlled potentiostat (CHI 910B, CH Instruments), and the scan rate was 100 mV/s. The probe solutions contained 1 mM potassium hexacyanoferrate(II) in 1 M KCl.

For the voltammetric detection of phospholipase A_2, solutions containing 10 μg/mL enzyme dissolved in 10 mM HEPES buffer saline (10 mM $CaCl_2$ and 100 mM NaCl, pH 7.7) were incubated with various SAM/lipid bilayers at room temperature for 30 min. After this step, the enzyme solutions were replaced by the same ferrocyanide solution as above, and voltammograms were then similarly obtained using gold covered with the enzyme-treated lipid films as the working electrode.

Impedance Analysis. Impedance spectroscopy measurements of aromatic thiol SAMs and the corresponding POPC/SAM hybrid structures were carried out on a Gamry electrochemical impedance analyzer system (Reference 600). Similar to the cyclic voltammetry setup, the Teflon cells hold a gold working electrode covered with a SAM or a bilayer, a platinum counter electrode, and a Ag/AgCl reference electrode. The electrolyte solution contains 10 mM KCl in DI water. During the impedance measurement, a 10 mV ac bias was applied, and its frequency was modulated from 10 to 10^4 Hz. Thus acquired impedance data were fitted to a Randles circuit using the modeling package included in Gamry Echem Analyst, which features a solution resistance component connected in series with the membrane-associated element containing a resistance and a capacitance component configured in parallel. The fitting results give the capacitance values of SAMs and hybrid bilayers. The capacitance of the lipid monolayer can be calculated from $C_{lipid}^{-1} = C_{BL}^{-1} - C_{SAM}^{-1}$, in which C represents the capacitance values of different films.[1] The thickness of these films was estimated from the relationship $1/C = d/\varepsilon\varepsilon_0$, in which d is the thickness of the dielectric medium separating the two conducting plates (i.e., the gold electrode and the electrolyte solution) and ε is the dielectric constant of the separating medium, which is 2.3 for C12 thiol,[3] 2.53 for biphenyl-4-thiol,[20] 2.54 for 2-naphthalenethiol,[20] 4.26 for thiophenol,[20] and 2.7 for POPC,[3] respectively. ε_0 is the permittivity of free space ($\varepsilon_0 \approx 8.85410 \times 10^{-12}$ F m^{-1}). All standard deviations were reported from three samples, with each sample measured three times.

Atomic Force Microscopy (AFM). A Bruker AFM system (MultiMode 8) was used for the morphological and mechanical characterization of aromatic thiol SAMs and phospholipid/thiol hybrid bilayers. Air and fluid sample holders from the same company were used for SAM and bilayer samples, respectively. All measurements were performed at room temperature. The thickness contrast between the phospholipid top layer and the bilayer in the buffer solution was obtained by scanning a 4 × 4 μm^2 bilayer in which a 1 × 1 μm^2 POPC patch was first removed in the center. To do so, a silicon nitride cantilever (MPP 12120-10, Bruker) with a nominated spring constant of 5 N/m and resonance frequency of 150 kHz was employed. In the first scratching run, the cantilever was operated in contact mode, where a relatively large force was obtained by setting the contact mode deflection set point to 2.5−4.5 V and the scan rate to 2−4 Hz. In the second scan, the AFM was switched to tapping mode, in which a larger area was imaged with the same tip at a scan rate of 1.0 Hz. The mechanical characteristics of SAMs were probed by operating the microscope in the peak force quantitative nanomechanical mapping (QNM) imaging mode in air using another probe (ScanAsyst-Air, Bruker, spring constant 0.4 N/m, resonance frequency 70 kHz). At the beginning of each measurement, the tip was calibrated for its deflection sensitivity. Images were recorded only after the peak force curves became stable. The modulus E^* was calculated by fitting the retract curve using the Derjaguin−Muller−Toporov (DMT) model.[21] All AFM images shown in Figure 4 were replotted with Gwyddion without any graphical modification or enhancement, whereas those in SI Figure 1 were flattened images generated by Bruker NanoScope Analysis 1.5.

RESULTS AND DISCUSSION

Four aromatic thiols are investigated in this study: thiophenol, 2-naphthalenethiol, biphenyl-4-thiol, and diphenylenevinylene (DPV) methanethiol, covering the smallest aromatic thiol (thiophenol) and three two-ring thiols of different structure and length (Figure 1). Compared to alkanethiols, SAMs formed by aromatic thiols often display less tilting on the gold surface, and their packing orientation also depends on the size and structure of thiols used.[14,15] In terms of the hydrophobicity of the resulting films, water contact angle measurements made by Rubinstein and co-workers[22] showed that SAMs of several

DOI: 10.1021/acs.langmuir.5b00476
Langmuir 2015, 31, 5228−5234

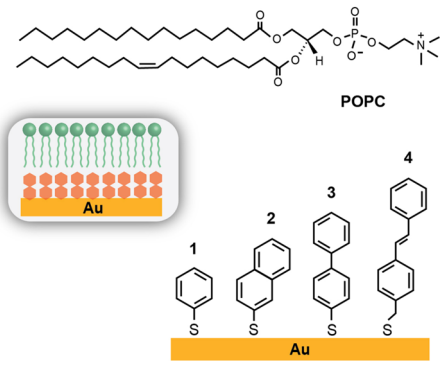

Figure 1. Schematic illustration of a hybrid bilayer consisting of an aromatic thiol monolayer self-assembled on a gold surface and a lipid monolayer. Aromatic thiols studied (**1** to **4**): thiophenol, 2-naphthalenethiol, biphenyl-4-thiol, and diphenylenevinylene methanethiol.

phenol thiols display significantly smaller angles as compared to SAMs formed by 1-octadecanethiol (C18 thiol). The lower packing density and association among aromatic thiols were further revealed by the observation that SAMs preformed by these aromatic thiols could be replaced by the C18 thiol. In the formation of a hybrid bilayer, these features may affect the deposition kinetics of lipids on these aromatic thiols as well as the mechanical, morphological, and electrical characteristics of the resulting structures. On the other hand, we chose zwitterionic 1-palmitoyl-2-oleoyl-*sn*-glycero-3-phosphocholine (POPC) as the single lipid component to avoid unnecessary complications at the beginning of this investigation. Owing to its low phase-transition temperature (−2 °C), the liposomal assemblies of POPC are expected to display a high fluidity at room temperature and hence a relatively low energy barrier for spreading and fusion when exposed to a hydrophobic surface.

Deposition of POPC on these aromatic SAMs was achieved by the liposome fusion method similar to the preparation of lipid/alkanethiol hybrid bilayers.[1] To test the packing integrity of these aromatic SAMs as well as the corresponding lipid-containing hybrid structures, we first examined the blocking of heterogeneous electron transfer of a small electroactive species by these films using cyclic voltammetry. As shown in Figure 2, because of the coverage of aromatic SAMs on the gold electrode, the oxidation of ferrocyanide in solution is significantly suppressed in all four cases. For the three shorter thiols in which the oxidation/reduction waves can still be discerned, this blocking effect is also manifested by an enlarged separation between the anodic and cathodic peaks. In comparison to results[22] on thiophenol and biphenyl-4-thiol reported by Rubinstein et al., the same SAMs presented here show a significantly stronger blocking effect, which should be due to the longer SAM formation time, i.e., overnight in our case vs 15 min to 2 h used by these authors. For SAMs alone, the degree of blocking roughly follows the size of the thiols: thiophenol < 2-naphthalenethiol < biphenyl-4-thiol < DPV. Here, even the most blocking one of this series, DPV, appears to be a less-efficient blocker than dodecanethiol (Figure 2, upper right panel), whereas the least blocking thiophenol forms still inferior barriers compared to the SAM and bilayer based on butanethiol (top vs bottom left panels). Interestingly, when a layer of POPC was deposited on top of these aromatic SAMs, all except the shortest thiophenol were able to block ferrocyanide oxidation nearly as well as the C12 thiol-based hybrid bilayer. These results clearly demonstrate that (1) lipids such as POPC can be equally well deposited on aromatic SAMs following the same procedure and (2) regardless of the exact

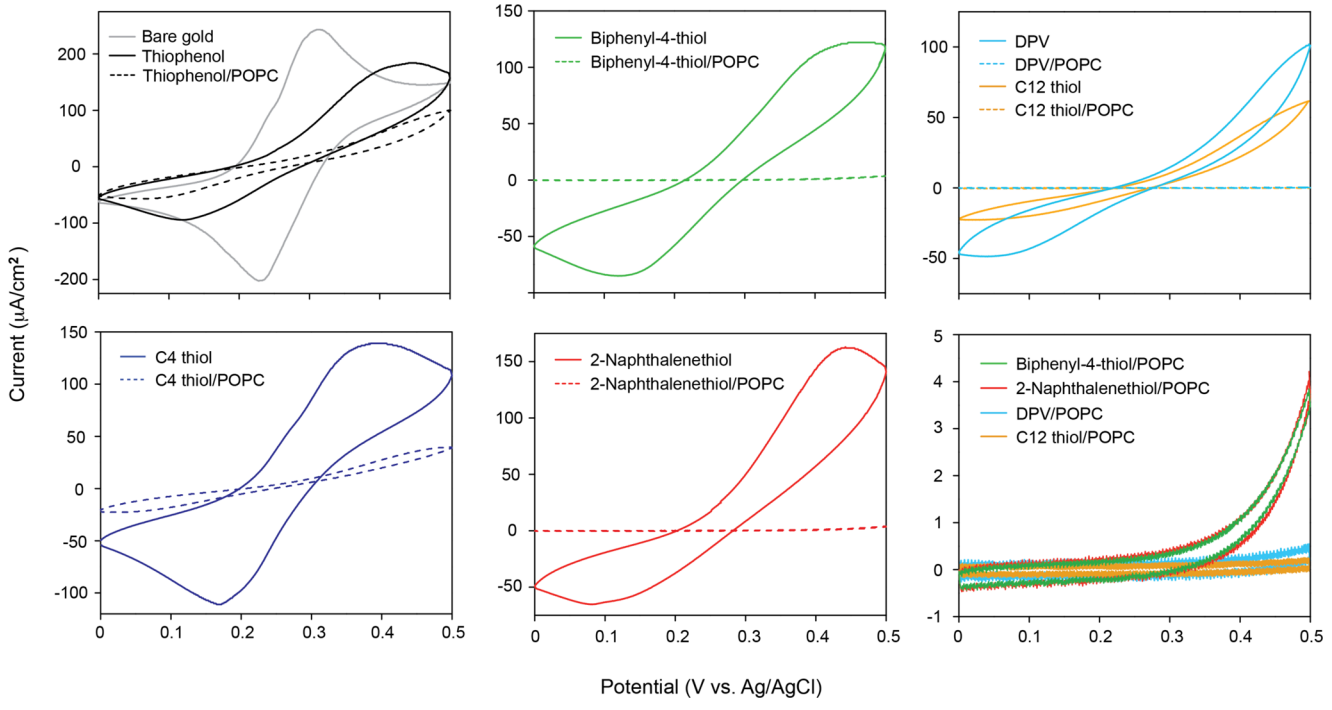

Figure 2. Cyclic voltammetric characterization of the formation of aromatic thiol SAMs (via the solid line) and the corresponding hybrid bilayers (via the dashed line) on gold. Voltammograms of C4- (bottom left panel) and C12-based (upper right panel) SAMs and bilayers are also included for comparison. Also included is the CV response from the bare gold surface of the same area (top left panel). All scans were conducted in 1.0 mM $Fe(CN)_6^{4-}$ in 1 M KCl aqueous solution, and the scan rate was 100 mV/s.

DOI: 10.1021/acs.langmuir.5b00476
Langmuir 2015, 31, 5228−5234

structure, thus-deposited lipids form a continuous and well-packed top layer that can effectively inhibit the permeation of small ions and thus move them further away from the underlying gold surface. In addition, these results reinforce previous observations[23−25] that continuous lipid layers can often form on defective, discontinuous, or curved surfaces. Underlying this high tolerance toward surface irregularities is the general and constant balance of various attractive and repulsive forces at the lipid/water interface.[10]

To gain more information about the structure of the lipid layer deposited on these aromatic SAMs, we next performed electrical impedance analysis on these films. Here, the attachment of a SAM or a hybrid bilayer to the gold surface significantly modifies the capacitance at the electrode/water interface and together with the solution resistance gives rise to distinctive impedance profiles characteristic of each film. As shown in Figure 3, top panel, the total impedance vs ac modulation frequency profiles of the four aromatic SAMs as well as their corresponding lipid hybrid structures can all be quantitatively reproduced by the Randles circuit model. In comparison, the same data can also be reasonably well fitted with a series R (solution)−C (membrane) model, with slightly but consistently inferior goodness-of-fit values (data not shown). From the fitting, one can then obtain the capacitance values associated with these membranes (Table 1). Here, the capacitance of the SAM decreases as its length increases, reflecting the fact that longer thiols extend the electrolytes further away from the underlying gold surface, which is in accord with the voltammetry data. By treating these SAMs as an ideal capacitor, one can further calculate the dielectric thickness of each SAM. Similarly, by considering the SAM and the lipid top layer as two capacitors configured in series, one can also estimate the thickness of the POPC layer. As shown in Table 1, except for thiophenol, a very consistent thickness of ∼1.2 nm was obtained for the lipid top layer deposited on the SAMs of the three longer thiols, thus suggesting single lipid monolayer formation on top of these aromatic SAMs. The calculated capacitance values of the POPC layer formed on the three long aromatic SAMs, ∼1.9 μF/cm^2, are well within the range of previous reports on the same lipid, e.g., 1.76 μF/cm^2 on C18 SAM[1] and 2.31 μF/cm^2 on C12 SAM.[26] The reason that such an agreement was not observed in the case of thiophenol is likely due to its small size and poor packing in the resultant SAM, which allows charge penetration and thus causes the ideal capacitor model to break down.

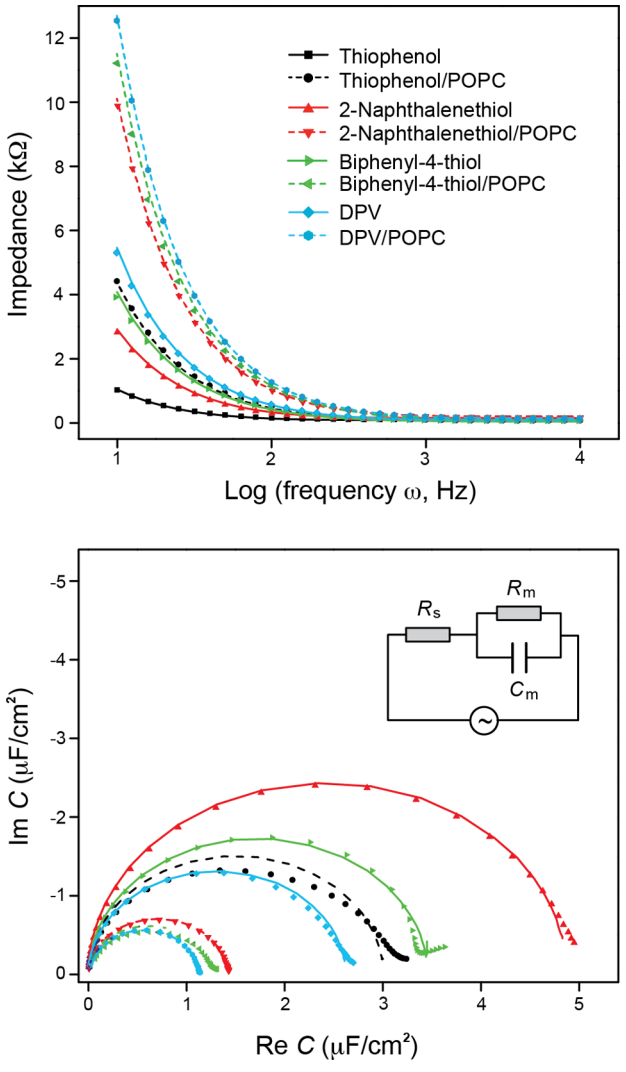

Figure 3. Impedance plots obtained from aromatic thiol SAMs (solid lines) and the corresponding hybrid bilayers (dashed lines) formed on gold. The supporting electrolytes contain 10 mM KCl in deionized water. The fitting results are modeled off the Randles circuit included in the figure and presented as solid/dashed lines, whereas the measured data are shown by various symbols. Not included in the bottom panel is the plot of the thiophenol SAM alone due to its significantly larger scale. See the Experimental Section for more details.

Plotting the real vs imaginary capacitance values associated with these films further yields the corresponding complex impedance spectra in semicircles (bottom panel, Figure 3). In all cases, the spectra start at the origin at high frequencies and tend to bend back and intercept the real-C axis at low frequencies, where the membrane capacitance dominates the overall impedance of the cell. The generally good agreement seen between measured and fitting data indicates that the employed circuit model adequately describes the impedance behaviors of these new hybrid bilayers, with thiophenol-based membranes again as the sole outlier.

Additional evidence corroborating the above conclusion is also obtained from AFM measurement of these new hybrid structures immersed in buffer. As shown in Figure 4, removing the top lipid layer from the underlying 2-naphthalenethiol SAM produces a negative pattern that is approximately 1.0 nm thick (measured valley to valley from the thickness profile), which compares well with the 1.2 nm feature similarly obtained from the C12 thiol-based hybrid bilayer. The roughness of the gold substrates, which is on the order of 0.3 nm, however, prevents us from drawing more quantitative conclusions regarding their relative thickness and thus the orientation of lipids deposited on these SAMs.

AFM nanomechanical mapping of these SAMs further revealed that a significant difference in elasticity exists among these organic thin films (Table 2). Of these, the C12 SAM displays the highest elastic modulus compared to the tested aromatic thiols, whereas the value associated with the biphenyl-4-thiol SAM is more than twice as high as that of 2-naphthalenethiol. These results point out the fact that the mechanical characteristics of SAMs are critically dependent on the structure, size, and packing density of the constituent thiols.

To explore the application potential of these aromatic/lipid hybrid bilayers and particularly features that may set these new structures apart from their alkanethiol-based counterparts, we

DOI: 10.1021/acs.langmuir.5b00476
Langmuir 2015, 31, 5228−5234

Table 1. Electrical Capacitance Values and Calculated Dielectric Thicknesses (in Parentheses) of Aromatic Thiol SAMs with/without POPC Deposited Atop

	capacitance of SAM (C_{SAM})[a]	capacitance of bilayer (C_{BL})[a]	capacitance of lipid layer (C_{lipid})[b]
thiophenol	13.55 ± 1.67 (0.28 ± 0.01)[c]	3.12 ± 0.1	4.05 (0.59)[c]
2-naphthalenethiol	4.89 ± 0.08 (0.46 ± 0.01)	1.40 ± 0.04	1.96 (1.22)
biphenyl-4-thiol	3.44 ± 0.09 (0.65 ± 0.01)	1.23 ± 0.03	1.91 (1.25)
DPV	2.58 ± 0.04	1.12 ± 0.04	1.96 (1.22)

[a]Values are obtained by fitting the impedance data with a Randles circuit model; units: $\mu F/cm^2$. [b]Calculated values in $\mu F/cm^2$. [c]Calculated thicknesses in nm. See the Experimental Section for more details.

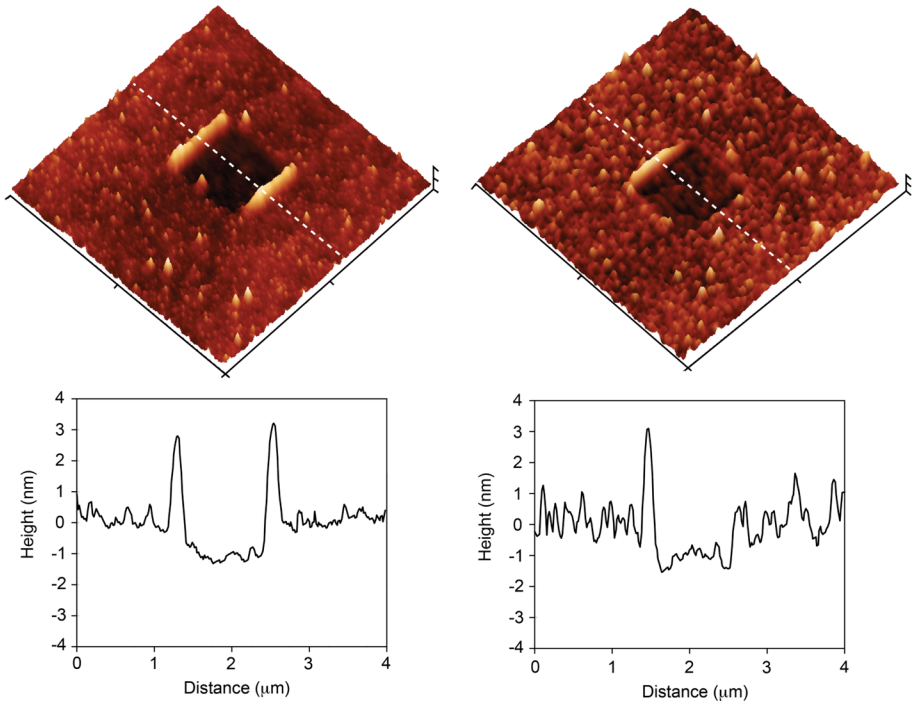

Figure 4. Top: AFM images of the 2-naphthalenethiol/POPC hybrid bilayer (right) as compared to that formed on the C12 SAM (left). Area scanned: 4 × 4 μm^2. To reveal the thickness of the top lipid layer, a 1 μm^2 lipid patch was first removed before imaging. See the Experimental Section for more details. Bottom: height profiles obtained from line scans (dashed lines) across the center of the corresponding images shown at the top.

Table 2. Mechanical Characteristics of 2-Naphthalenethiol and Biphenyl-4-thiol SAMs as Compared to Those of C12 SAM

	DMT modulus (MPa)	rms (MPa)
2-naphthalenethiol	374.7	23.7
biphenyl-4-thiol	856.6	232.4
C12 thiol	1722.0	496.3

next designed and examined a biorecognition scheme in which a lipolytic enzyme, phospholipase A_2, was detected voltammetrically on these hybrid lipid bilayers. As shown in Figure 5, this enzyme specifically hydrolyzes the *sn*-2 acyl bond of a phospholipid, (i.e., POPC as the case here), producing its corresponding free fatty acid and lysophospholipid.[27,28] Significantly, treating the 2-naphthalenethiol/POPC bilayer with phospholipase A_2 nearly completely restores the oxidation of ferrocyanide directly obtained from the corresponding SAM alone (Figure 2), which demonstrates that this enzyme can effectively hydrolyze phospholipids packed in a planar hybrid bilayer. Moreover, the accompanying cathodic wave is noticeably larger than that from the SAM alone, suggesting that the enzyme treatment produces a restructured lipid surface rather than a complete removal of the lipids from the SAM. From a biosensor's perspective, interestingly, superior sensitivity can be obtained with the aromatic/lipid bilayer as compared to its alkane/lipid counterparts. In the case of the bilayer based on butanethiol, specifically, the low sensitivity is caused by the relatively large voltammetric response from its bilayer, which translates to a large background noise. For the longer C12-based structure, on the other hand, the sensitivity is extremely poor because the film after the enzyme treatment remains almost as blocking as the starting bilayer, rendering this bilayer rather ineffective in the detection of the enzyme (Figure 5, voltammograms in orange). By contrast, optimal detection is achieved by the aromatic-based bilayer because as a whole this bilayer still functions as an adequate mass-transfer barrier to the redox probe in solution (i.e., low background), and more importantly, the top lipid layer contributes predominantly to the blocking of electron transfer, whose hydrolysis and restructuring thus produce a high voltammetric signal. Consequently, it is the large difference in the blocking of heterogeneous electron transfer displayed by the two types of hybrid lipid bilayers on which our biorecognition mechanism is based.

The different voltammetry responses shown by the two types of hybrid bilayers are necessarily a result of some structural change in the deposited lipids caused by the enzyme treatment,

DOI: 10.1021/acs.langmuir.5b00476
Langmuir 2015, 31, 5228−5234

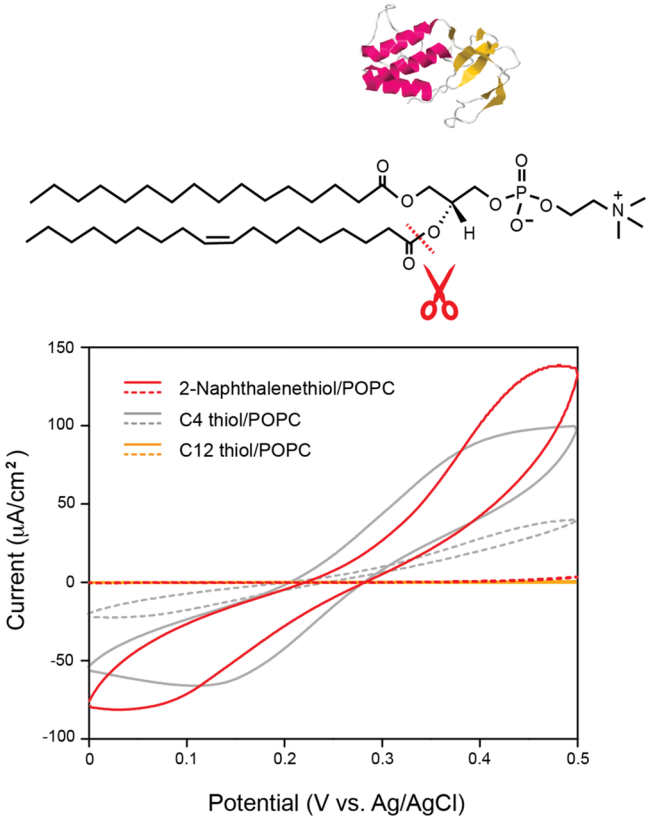

Figure 5. Cyclic voltammetric detection of phospholipase A_2 using the 2-naphthalenethiol/POPC hybrid bilayer. The CV responses were obtained from 1.0 mM $Fe(CN)_6^{4-}$ in 1 M KCl before (dashed line) and after (solid line) the bilayer was incubated in 10 μg/mL phospholipase A_2 for 30 min. The same operation was also run on the C4/POPC and C12/POPC bilayers for comparison. The structure (PDB 1POC) of this enzyme and its cleavage site on phospholipids are shown at the top.

which can be understood as follows. To begin with, the enzymatic hydrolysis alters the chemical and structural identities of the lipid monolayer, which break the balance of various forces at the lipid/water interface and therefore may potentially trigger a morphological change and loss of material in the lipid layer. Because both reaction products are more water-soluble than the starting lipid, they display a higher tendency to leave for the aqueous phase. Considering the packing geometry, moreover, the hydrolysis converts the rod-shaped POPC for which the lamellar organization represents the most stable structure to its lysophospholipid and fatty acid, whose energetically favored assemblies are the regular and inverted micelles, respectively. Before the departure of these lipid derivatives from the lipid/water interface can occur, however, another energy price has to be paid for them to overcome the hydrophobic/hydrophobic attraction executed by the SAM underneath. Indeed, such an energy barrier can be so high for long-chained lipids that the cleaved products remain associated with the bilayer.[29] This nondeparture of lipids explains the CV of C12-based bilayers upon enzyme treatment, in which the observed oxidation current is actually less than that of its SAM alone (Figure 2). By contrast, the aromatic SAMs pose less hydrophobic drag toward the acyl chains of the lipids (e.g., based on contact angle measurements)[22] and hence a lower energy barrier for the lipid products to desorb from the surface. As the lipid desorption proceeds, the underlying SAM is once again directly exposed to the aqueous phase, which serves to recover the voltammetric response of the aromatic SAM itself. Our preliminary AFM imaging results (SI Figure 1) appear to support this analysis. While the images of POPC/C12 SAM bilayers obtained before and after the enzyme treatment display little difference, imaging the NPT-based bilayer upon enzyme incubation consistently reveals irregular stripes that can be attributed to the partial removal of the top lipid layer. The typical height of these new features, ~3 nm, however, is greater than the thickness of the POPC layer indicated by our lipid scratching measurements (Figure 4), which could be due to either the adsorbed enzymes or the readsorption of cleaved lipids. Further examination is clearly needed in order to put our interpretation on a more robust footing.

CONCLUSIONS

We have established here that lipid monolayers can be reliably deposited on self-assembled aromatic thiols to give rise to a new family of hybrid bilayers. New biomembrane models and biorecognition strategies may be developed from these new structures by exploring the rich structural varieties and novel electronic properties of aromatic thiols. To demonstrate such possibilities, we show here that a lipolytic enzyme can be detected more sensitively using these phospholipid/aromatic thiol bilayers. Continuing along this direction, our follow-up research will be directed toward the identification of potential trends in electrochemical behaviors of bilayers based on aromatic thiols of different size and structure as well as developing these structures into new biomimicking photoconversion systems.[13,26]

ASSOCIATED CONTENT

Supporting Information

AFM images of hybrid bilayers after the enzyme treatment. The Supporting Information is available free of charge on the ACS Publications website at DOI: 10.1021/acs.langmuir.5b00476.

AUTHOR INFORMATION

Corresponding Author

*E-mail: wzz0001@auburn.edu. Tel: 334-844-6984.

Notes

The authors declare no competing financial interest.

ACKNOWLEDGMENTS

This work is supported by the National Science Foundation (award no. CHE-0951743). The atomic force microscope used in this work was funded by a level-4 IGP award from the Office of the Vice President for Research and Economic Development of Auburn University. We thank Prof. J. Gorden for his assistance with the synthesis and characterization of diphenylenevinylene methanethiol.

REFERENCES

(1) Plant, A. L. Self-Assembled Phospholipid/Alkanethiol Biomimetic Bilayers on Gold. *Langmuir* **1993**, *9*, 2764−2767.

(2) Plant, A. L. Supported Hybrid Bilayer Membranes as Rugged Cell Membrane Mimics. *Langmuir* **1999**, *15*, 5128−5135.

(3) Silin, V. I.; Wieder, H.; Woodward, J. T.; Valincius, G.; Offenhausser, A.; Plant, A. L. The Role of Surface Free Energy on the Formation of Hybrid Bilayer Membranes. *J. Am. Chem. Soc.* **2002**, *124*, 14676−14683.

DOI: 10.1021/acs.langmuir.5b00476
Langmuir 2015, 31, 5228−5234

(4) Steinem, C.; Janshoff, A.; Ulrich, W.-P.; Sieber, M.; Galla, H.-J. Impedance Analysis of Supported Lipid Bilayer Membranes: A Scrutiny of Different Preparation Techniques. *Biochim. Biophys. Acta* **1996**, *1279*, 169−180.
(5) Twardowski, M.; Nuzzo, R. G. Molecular Recognition at Model Organic Interfaces: Electrochemical Discrimination Using Self-Assembled Monolayers (SAMs) Modified via the Fusion of Phospholipid Vesicles. *Langmuir* **2003**, *19*, 9781−9791.
(6) Castellana, E. T.; Cremer, P. S. Solid Supported Lipid Bilayers: From Biophysical Studies to Sensor Design. *Surf. Sci. Rep.* **2006**, *61*, 429−444.
(7) Cooper, M. A. Advances in Membrane Receptor Screening and Analysis. *J. Mol. Recognit.* **2004**, *17*, 286−315.
(8) Hubbard, J. B.; Silin, V.; Plant, A. L. Self Assembly Driven by Hydrophobic Interactions at Alkanethiol Monolayers: Mechanism of Formation of Hybrid Bilayer Membranes. *Biophys. Chem.* **1998**, *75*, 163−176.
(9) Seifert, U.; Lipowsky, R. Adhesion of Vesicles. *Phys. Rev. A* **1990**, *42*, 4768−4771.
(10) Israelachvili, J. N. *Intermolecular and Surface Forces*, 3rd ed.; Elsevier Inc.: Amsterdam, 2011; Chapter 20.
(11) Elliott, J. T.; Burden, D. L.; Woodward, J. T.; Sehgal, A.; Douglas, J. F. Phospholipid Monolayers Supported on Spun Cast Polystyrene Films. *Langmuir* **2003**, *19*, 2275−2283.
(12) Howland, M. C.; Sapuri-Butti, A. R.; Dixit, S. S.; Dattelbaum, A. M.; Shreve, A. P.; Parikh, A. N. Phospholipid Morphologies on Photochemically Patterned Silane Monolayers. *J. Am. Chem. Soc.* **2005**, *127*, 6752−6765.
(13) Xie, H.; Jiang, K.; Zhan, W. Modular Molecular Photovoltaic System Based on Phospholipid/Alkanethiol Hybrid Bilayers: Photocurrent Generation and Modulation. *Phys. Chem. Chem. Phys.* **2011**, *13*, 17712−17721.
(14) Love, J. C.; Estroff, L. A.; Kriebel, J. K.; Nuzzo, R. G.; Whitesides, G. M. Self-Assembled Monolayers of Thiolates on Metals as a Form of Nanotechnology. *Chem. Rev.* **2005**, *105*, 1103−1169.
(15) Frey, S.; Stadler, V.; Heister, K.; Eck, W.; Zharnikov, M.; Grunze, M. Structure of Thioaromatic Self-Assembled Monolayers on Gold and Silver. *Langmuir* **2001**, *17*, 2408−2415.
(16) Käfer, D.; Witte, G.; Cyganik, P.; Terfort, A.; Wöll, C. A Comprehensive Study of Self-Assembled Monolayers of Anthracenethiol on Gold: Solvent Effects, Structure and Stability. *J. Am. Chem. Soc.* **2006**, *128*, 1723−1732.
(17) Dudek, S. P.; Sikes, H. D.; Chidsey, C. E. D. Synthesis of Ferrocenethiols Containing Oligo(phenylenevinylene) Bridges and Their Characterization on Gold Electrodes. *J. Am. Chem. Soc.* **2001**, *123*, 8033−8038.
(18) Fan, F.-R. F.; Yao, Y.; Cai, L.; Cheng, L.; Tour, J. M.; Bard, A. J. Structure-Dependent Charge Transport and Storage in Self-Assembled Monolayers of Compounds of Interest in Molecular Electronics: Effects of Tip Material, Headgroup, and Surface Concentration. *J. Am. Chem. Soc.* **2004**, *126*, 4035−4042.
(19) Zhan, W.; Jiang, K. A Modular Photocurrent Generation System Based on Phospholipid-Assembled Fullerenes. *Langmuir* **2008**, *24*, 13258−13261.
(20) *CRC Handbook of Chemistry and Physics*, 85 ed.; Lide, D. R., Ed.; online version 2005, http://www.hbcpnetbase.com; CRC Press: Boca Raton, FL, 2005.
(21) Young, T. J.; Monclus, M. A.; Burnett, T. L.; Broughton, W. R.; Ogin, S. L.; Smith, P. A. The Use of the PeakForce Quantitative Nanomechanical Mapping AFM-Based Method for High-Resolution Young's Modulus Measurement of Polymers. *Meas. Sci. Technol.* **2011**, *22*, 125703.
(22) Sabatani, E.; Cohen-Boulakia, J.; Bruening, M.; Rubinstein, I. Thioaromatic Monolayers on Gold: A New Family of Self-Assembling Monolayers. *Langmuir* **1993**, *9*, 2974−2981.
(23) Tanaka, M.; Sackmann, E. Polymer-Supported Membranes as Models of the Cell Surface. *Nature* **2005**, *437*, 656−663.
(24) White, R. J.; Ervin, E. N.; Yang, T.; Chen, X.; Daniel, S.; Cremer, P. S.; White, H. S. Single Ion-Channel Recordings Using Glass Nanopore Membranes. *J. Am. Chem. Soc.* **2007**, *129*, 11766−11775.
(25) Jönsson, P.; Jonsson, M. P.; Höök, F. Sealing of Submicrometer Wells by a Shear-Driven Lipid Bilayer. *Nano Lett.* **2010**, *10*, 1900−1906.
(26) Jiang, K.; Xie, H.; Zhan, W. Photocurrent Generation from $Ru(bpy)_3^{2+}$ Immobilized on Phospholipid/Alkanethiol Hybrid Bilayers. *Langmuir* **2009**, *25*, 11129−11136.
(27) Cherney, D. P.; Myers, G. A.; Horton, R. A.; Harris, J. M. Optically Trapping Confocal Raman Microscopy of Individual Lipid Vesicles: Kinetics of Phospholipase A_2-Catalyzed Hydrolysis of Phospholipids in the Membrane Bilayer. *Anal. Chem.* **2006**, *78*, 6928−6935.
(28) Jackman, J. A.; Cho, N.-J.; Duran, R. S.; Frank, C. W. Interfacial Binding Dynamics of Bee Venom Phospholipase A_2 Investigated by Dynamic Light Scattering and Quartz Crystal Microbalance. *Langmuir* **2010**, *26*, 4103−4112.
(29) Mirsky, V. M.; Mass, M.; Krause, C.; Wolfbeis, O. S. Capacitive Approach To Determine Phospholipase A_2 Activity toward Artificial and Natural Substrates. *Anal. Chem.* **1998**, *70*, 3674−3678.

DOI: 10.1021/acs.langmuir.5b00476
Langmuir 2015, 31, 5228−5234